BIOMIMETIC BIDIRECTIONAL SWITCHABLE ADHESIVE INSPIRED BY THE GECKO

Noshir Pesika, Associate Professor, Tulane University, New Orleans, LA

Introduction

The complex anisotropic and hierarchical structure of the gecko provides a compliant surface with an effective modulus of ~100 KPa[3] although the setal structures are composed of relatively hard β-keratin (~1-2 GPa). The resulting compliance allows for the thin terminal structures of the setae and spatula pads to come into intimate contact with opposing surfaces, which maximizes the attractive weak, short-ranged van der Waals interactions required for high adhesion (~1 N/cm^2) and friction (~10 N/cm^2) forces. The anisotropic adhesion of gecko pads originates from the fact that the setae are tilted at an angle of ~45°.[4] Several types of gecko-like adhesive materials have been developed over the last decade, [5-12] yet a true mimic still remains elusive because of limitations in current surface nanofabrication techniques as well as limitations involved in incorporating gecko-like adhesives into devices that offer proper articulation. In 2003, Geim et al.[5] were the first to microfabricate a gecko-like material out of a soft polymer, although the latter did not possess anisotropic adhesive properties and required relatively large preloads (i.e., the force applied after contact) to activate the adhesion. New developments in the fabrication of gecko-like adhesives included the addition of tilt to the structures,[13-15] using carbon nanotubes,[16, 17] introducing angled mushroom tips,[18] functionalizing the gecko-like surface with mussel adhesive proteins,[19] using surface strains[20] or shear[21] to tune adhesion. Other polymer-based structures have been developed[22] although they lack the property of shear-induced adhesion (i.e., the maximum adhesion and friction forces are only attained upon shearing the surface whereas without shear, the adhesive shows minimal adhesion forces) or required relatively large normal pressures to activate the release mechanism[23]. Recently, our group developed a general approach to easily incorporate a desired tilt angle into gecko-like fibrillar structures,[24] and the resulting gecko-like surface was reminiscent of the tribological properties of gecko pads. With our current design, the structures show anisotropic adhesion and friction properties even in the absence of tilt in the structures although adding tilt to the structures does increase the magnitude of both friction and adhesion for gripping.

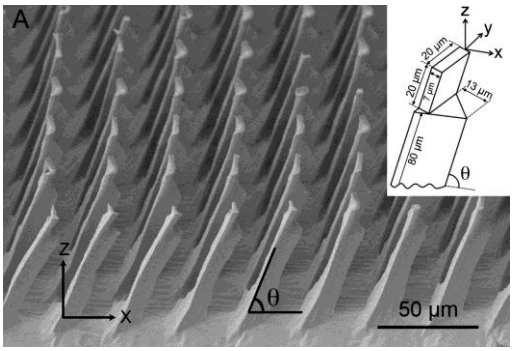

Figure 1. SEM image of a gecko-inspired adhesive consisting of tilted prismatic pillars with a first level of triangular prism structures and a second level of thinner rectangular adhesion pads biased towards one of the flat edges. The inset is a schematic illustration of the terminal end of a prismatic pillar.

Here, we introduce a new generation of polyurethane-based gecko-like structures (hereafter referred to as "prismatic" pillars), consisting of 2 levels of hierarchy (**Figure 1**); a triangular prism base (30 µm x 25 µm x 25 µm, and 80 µm high) terminated by a rectangular tip (20 µm x 20 µm x 7 µm), arranged in a rectangular lattice (30 µm center-to-center in the tilt (x-axis) direction, and 37 µm center-

to-center along the in-plane or y-axis). Through proper articulation (i.e., to activate either gripping or releasing) of the prismatic gecko-inspired adhesive, we obtain anisotropic frictional-adhesive properties, which allow for reversible attachment and detachment over multiple cycles.

Result and discussion

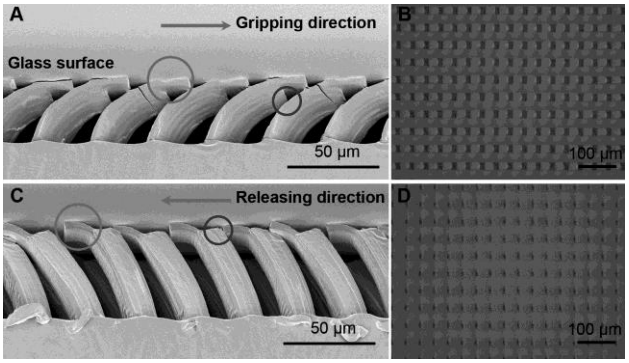

Figure 2. (A) In the gripping direction, a large contact area (larger circle) is formed between the adhesive pads and the opposing surface. The apexes of the triangular prisms (smaller circle) prevent large area contacts between neighboring pillars. (C) In the releasing direction, a smaller contact area is formed between the adhesive and the opposing surface (larger circle). The apexes of the triangular prisms (smaller circle) prevent large area contacts between the adhesive pads and opposing surface. (B, D) Optical microscope images of the gecko-inspired surfaces sheared against a transparent glass microscope slide in the gripping direction, and releasing direction, showing the very different anisotropic contact areas formed between the adhesive pads and the glass surface.

Scanning electron microscope (SEM) images of the prismatic surface sheared in the gripping and releasing directions demonstrate the anisotropic effects of the judicious prismatic pillar design. In the gripping direction, a large contact area is formed between the adhesive pads and the opposing surface (larger circle in **Figure 2A**). In addition, the apex of the triangular prism only allows for a point contact between neighboring pillars (smaller circle in Figure 2A) thus minimizing nearest neighbor adhesion. The latter is essential to allow the pillars to elastically regain their original configuration when they are unloaded. If the adhesive interactions between neighboring pillars cannot be overcome by the stored elastic energy (within the pillars), self-matting or clumping occurs[25] (i.e., the pillars remain stuck to each other), which is undesirable.

In the releasing direction, the apex of each triangular prism (smaller circle in **Figure 2C**) now serves to prevent the adhesive pads from forming good contact with the opposing surface (larger circle in Figure 2C). Corresponding top-view optical microscope images of the prismatic pillars under shear against a transparent microscope glass slide in the gripping and the releasing directions (**Figure 2B, D**) also confirm the anisotropic contact mechanics of our structures. The large contact area between the adhesive pads and the glass surface generated in the gripping direction (Figure 2B) allows for both high friction and adhesion forces. The latter pin the adhesive pads to the opposing surface and upon further shearing leads to small peeling angles in the bifurcation region between the adhesive pads and the opposing surface, which enhances the adhesion forces.[26, 27] By contrast, in the releasing direction (Figure 2D), a relatively small contact area is formed between the adhesive pads and the glass surface thus reducing both the friction and adhesion forces. Upon further shearing, the small friction forces are not sufficient to pin the adhesive pads, and sliding or detachment occurs.

Figure 3 shows the tribological properties of a tilted prismatic surface (tilt angle θ=63° in the unloaded state) sheared in the gripping direction. In a typical experiment, a preload of 50 mN was

applied for 5 s, followed by shearing of the opposing flat borosilicate glass surface. Upon shearing, the normal load $F_{\perp}$ entered the adhesive regime and the friction force $F_{\parallel}$ increased. The glass surface was then retracted perpendicularly until it detached at the maximum adhesive (pull off) force of $F_{\perp} \approx$ 500 mN. The relatively large ratio of the adhesion force to the applied preload force of 10 (i.e., 500/50) is particular attractive for climbing robots whereby low preloads allow for robust and efficient locomotion on vertical and inverted horizontal surfaces.[28, 29] Data for the maximum adhesion $F_{\perp}$ and the maximum friction $F_{\parallel}$ forces on pull-off were recorded for 30 cycles (Fig. 3B) for 2 different samples: one with a tilt angle of θ=63°, the other with no tilt (θ=90°). The results show the influence of the tilt angle θ on the adhesion and friction forces, and also demonstrate the reusability of this gecko-like adhesive structure.

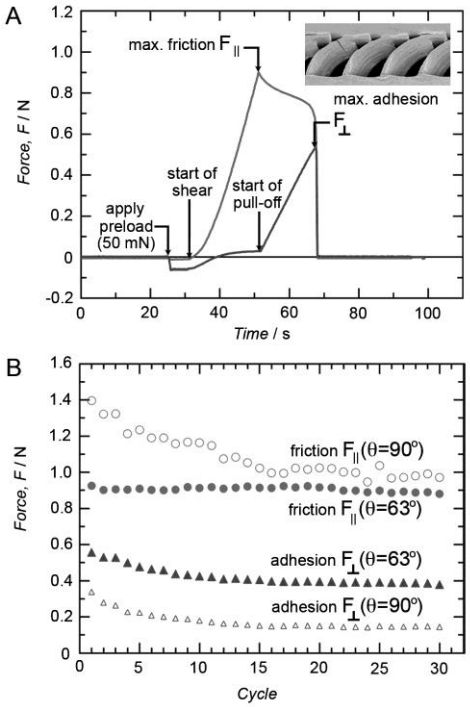

Figure 3. (A) Plot of the adhesion $F_{\perp}$ and friction $F_{||}$ forces generated during a typical measurement in the gripping direction. (B) Plot of the maximum friction force ($F_{||}$) and maximum adhesion (pull-off) force ($F_{\perp}$) over 30 cycles for vertical (θ=90°) and tilted (θ=63°) pillars. The preload was 50 mN. The shearing and pull-off velocities were both 10 μm/s.

According to the peel zone model[27] for tape peeling, smaller peel angles between the adhesive pads and the opposing surface lead to larger adhesion and friction forces because of the larger interaction area in the bifurcation region of the peeling surfaces. Our data is consistent with the peel zone model: pillars that had no tilt (θ=90°) produced smaller adhesion forces compared to the pillars with tilt. We also found that the maximum friction force was larger for the pillars with tilt compared to those without tilt (Supplementary Figures 1 and 2), again consistent with the peel zone model. The lower friction forces recorded for the pillars with tilt in Figure 3B is because in these experiments the surfaces were sheared only to the point of the maximum adhesion (pull-off) force which did not coincide with the maximum friction force (Supplementary Figure 2). We also found a monotonic decrease in both the adhesion and friction forces within the first 15 cycles. We attribute this decrease to material (i.e., polymer) transfer from the prismatic surface to the glass probe as recently characterized by Kroner et al.[30]

Similarly, the tribological properties of the prismatic surface were measured while shearing in the gripping direction, followed by shearing in the releasing direction, and finally pulling off to simulate the detachment process (**Figure 4**). The maximum adhesion force $F_{\perp}$ in the releasing direction was lower than in the gripping direction. The magnitude of the friction force $F_{||}$ in the releasing direction was also found to be considerably lower than in the gripping direction (cf. $F_{||}$~0.9 N in the gripping direction versus ~0.13 N in the releasing direction).

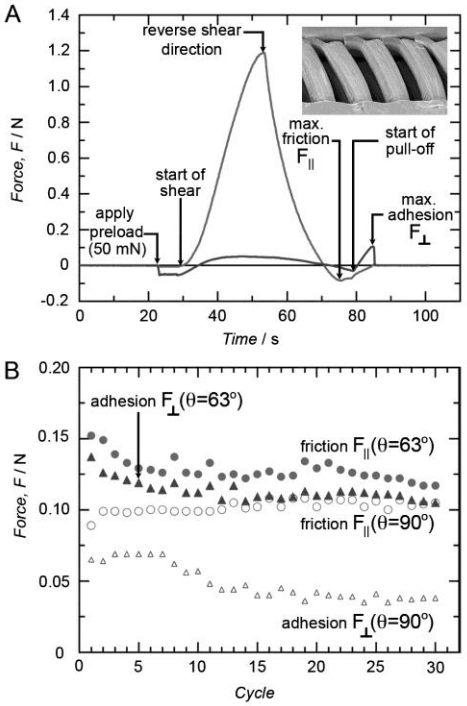

Figure 4. (A) Plot of the adhesion $F_{\perp}$ and friction $F_{||}$ forces generated during a typical measurement in the releasing direction. Each measurement cycle consisted of first shearing in the gripping direction followed by shearing in the releasing direction, before detachment. (B) Plot of the maximum friction force ($F_{||}$) and maximum adhesive pull-off force ($F_{\perp}$) over 30 cycles for vertical (θ=90°) and tilted (θ=63°) prismatic pillars. The preload was 50 mN. The shearing and pull-off velocities were both 10 μm/s.

To demonstrate the practical applications of the prismatic surface, two configurations were tested to suspend weights on vertical and horizontal surfaces, thus simulating walls and ceilings. **Figure 5A** shows the first configuration, which exploits primarily the friction forces generated by the prismatic surface to hold a 450 g weight against a vertical glass slide. An upward stroke of the prismatic surface (relative to the glass surface) would cause detachment.

In the horizontal configuration (**Figure 5B**), a sliding stage was fabricated to apply and maintain a lateral shear force on the prismatic surface in the gripping direction allowing for a large adhesion force to be generated in the vertical direction. Reversing the lateral shear force would cause detachment. To our knowledge, this is the first demonstration of using a gecko-like adhesive with shear-induced adhesion and friction properties to hold weights from inverted (ceiling-like) horizontal surfaces. In both cases, the weights have remained suspended for over 4 weeks.

A potential application for these switchable gecko-like adhesives involves moving delicate parts (e.g., electronic parts or computer chips) in assembly lines without using mechanical gripping or leaving a residue on the parts.

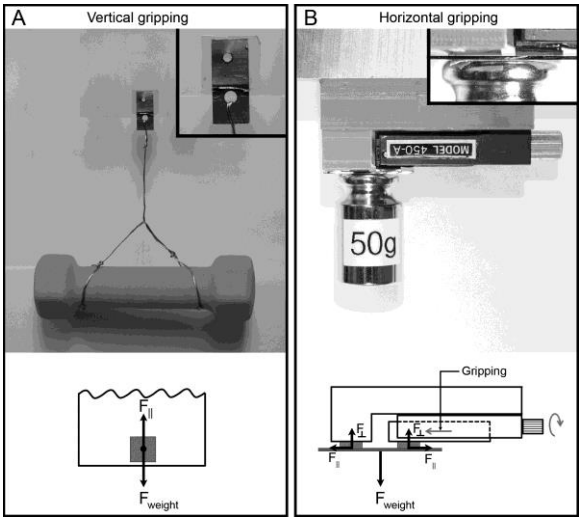

Figure 5. (A) Optical image of a 450 g weight supported from a vertical glass microscope slide using a prismatic surface of area ≈ 2 cm^2. Friction forces ($F_{||}$) are predominantly used in this configuration. An upward stroke of the prismatic surface would cause the weight to detach. (B) Optical image of a 50 g supported from a horizontal silicon wafer using a prismatic surface of area ≈ 1.6 cm^2. Corresponding schematic illustrations are shown below each image. In the horizontal gripping configuration, (B), the shear motion of the slider (red arrow) was used to generate the friction forces ($F_{||}$) that activated the adhesion forces ($F_{\perp}$) to hold the weight. Reversing the shear direction would cause the weight to detach. The weights have been hanging for several weeks.

Our current generation of gecko-like adhesive surfaces (i) possess required anisotropic tribological properties, (ii) provide relatively large adhesion and friction forces in the gripping direction, (iii) require relatively small preloads to activate the strong adhesion, (iv) require weak opposing forces or motions to detach, and (v) are reusable over multiple cycles. Nevertheless, additional studies and improvements are needed to develop a true gecko adhesive mimic. Typical natural or synthetic surfaces are rarely smooth and clean (such as the silicon wafers or microscope glass slides used in our studies), and ambient contamination may be present. We are currently studying the influence of surface roughness on the performance of our prismatic surfaces, and although they do not posses a self-cleaning property, we are able to recover the initial high adhesion and friction by rinsing the prismatic surface with deionized water and allowing it to dry. Our new design of prismatic structures opens the way for new gecko-like adhesive surfaces that do not rely on intensive nanofabrication but rather on judicious engineering of surface microstructures and proper articulation of the surfaces.

Experimental

Fabrication of patterned silicon mold

Silicon master wafers were fabricated using standard microfabrication techniques. Briefly, 4 in. silicon wafers (test grade, University Wafers) were cleaned in an oxygen plasma, after which a 600 nm oxide layer was grown using plasma-enhanced chemical vapor deposition. Next, positive photoresist (Shipley 1813, MicroChem Corp.) was spun onto the wafers, patterned with rectangular structures mimicking the gecko spatulae, and developed. The oxide layer was then etched by reactive ion etching with CF_4. The patterned oxide layer formed the bottom of the two-layer etch mask. The remaining photoresist was stripped off, and a new layer of photoresist (Shipley 1818, MicroChem Corp.) was spun onto the wafers. This new layer was patterned with the triangular prismatic structures mimicking the gecko setae, and developed. The photoresist layer formed the top of the two-layer etch mask. Once the

two-layer etch mask was in place, the hierarchical structure itself was formed using deep reactive ion etching. First, the wafer was etched to a depth of 80 μm. The photoresist was then stripped from the wafer, revealing the bottom layer (oxide) etch mask. The wafer was then etched an additional 20 μm to form the final rectangular pad structure.

Fabrication of prismatic dry adhesive

Two-level hierarchical polyurethane (PU) based (ST-1060 BJB Enterprise, Inc., Tustin, CA) dry adhesives were fabricated in a multi-step process as previously described[24]. Briefly, in the first step, a silicon master wafer was used as a mold to create an inverse polydimethylsiloxane (PDMS) replica. To facilitate the peeling of the PDMS inverse mold from the silicon master, the latter was pretreated with a self-assembled monolayer of octadecyltrichlorosilane (OTS) coating. Sylgard 184 PDMS (Dow Corning, Midland, MI) was mixed in a 10:1 (pre-polymer/cross-linker) ratio. After removal of air bubbles formed during mixing, the viscous liquid was poured onto the silicon master and cross-linked at 75 °C for 40 min. The partially cured PDMS replica was then laterally sheared in a home-built shearing device by applying a predetermined shear distance to achieve the desired tilt angle (ranging from 60°to 90°). The PDMS replica was then fully cured in its sheared state at 75 °C for 24 h, resulting in the PDMS replica mold with tilted triangular holes and tips. PU was then poured onto the PDMS replica and allowed to cure at 75 °C for 72 h. The final PU-based dry adhesive was peeled off from the PDMS replica.

Characterization of tribological properties

Adhesion and friction measurements were performed on a universal materials tester (CETR Enterprise, Inc., Campbell, CA). A flat 2 cm x 2 cm borosilicate glass surface, attached to a force sensor (DFM, CETR Enterprise, Inc., Campbell, CA) with a cantilever (spring constant $k \approx 4000$ N/m), was then brought into contact with the prismatic gecko-like surface at a predetermined preload. During a typical experiment, the glass surface was brought into contact with the sample with a preload of 50 mN. The glass surface was dragged in the gripping direction at a velocity of 10 μm/s after which it was pulled off at 90° from the sample at the same speed. For the detachment experiments, after shearing in the gripping direction (to activate the adhesion), the glass surface was then dragged in the opposite (releasing) direction and pulled off at 90° from the sample. Samples with tilt angles θ of 90° (i.e., no tilt) and 63° were tested to study the influence of the tilt angle. Prior to each experiment, the glass surface was cleaned with ethanol while the samples were tested without pre-cleaning.

References

[1] K. Autumn, Y. A. Liang, S. T. Hsieh, W. Zesch, W. P. Chan, T. W. Kenny, R. Fearing, R. J. Full, *Nature.* **2000**, *405*, 681.

[2] K. Autumn, A. Dittmore, D. Santos, M. Spenko, M. Cutkosky, *J. Exp. Bio.* **2006**, *209*, 3569.

[3] K. Autumn, C. Majidi, R. E. Groff, A. Dittmore, R. Fearing, *J. Exp. Bio.* **2006**, *209*, 3558.

[4] N. Pesika, N. Gravish, M. Wilkinson, B. X. Zhao, H. B. Zeng, Y. Tian, J. Israelachvili, K. Autumn, *J. Adhesion* **2009**, *85*, 512.

[5] A. K. Geim, S. V. Dubonos, I. V. Grigorieva, K. S. Novoselov, A. A. Zhukov, S. Y. Shapoval, *Nature Materials* **2003**, *2*, 461.

[6] N. J. Glassmaker, A. Jagota, C. Y. Hui, J. Kim, *J. R. Soc. Inter.* **2004**, *1*, 23.

[7] C. Greiner, D. A. Campo, E. Artz, *Langmuir* **2007**, *23*, 3495.

[8] D. Sameoto, C. Menon, *J. Micromech. Microeng.* **2010**, *20*, 115037.

[9] T. S. Kustandi, V. D. Samper, D. K. Yi, W. S. Ng, P. Neuzil, *Adv. Func. Mater.* **2007**, *17*, 2211.

[10] J. Yu, S. Chary, S. Das, J. Tamelier, K. L. Turner, J. N. Israelachvili, *Langmuir* **2012**, *28*, 11527.

[11] S. Reddy, E. Arzt, D. A. Campo, *Adv. Mater.* **2011**, *19*, 3010.

[12] H. Lee, B. Bhushan, *J. Coll. Inter. Sci.* **2012**, *372*, 231.

[13] M. P. Murphy, B. Aksak, M. Sitti, *Small* **2009**, *5*, 170.

[14] J. Lee, R. S. Fearing, K. Komvopoulos, *Appl. Phys. Lett.* **2008**, *93*, 191910.
[15] H. E. Jeong, J. Lee, H. N. Kim, S. H. Moon, K. Y. Suh, *PNAS* **2009**, *106*, 5639.
[16] B. Yurdumakan, N. R. Raravikar, P. M. Ajayan, A. Dhinojwala, *Chem. Comm.* **2005**, *30*, 3799.
[17] L. Qu, L. Dai, M. Stone, Z. Xia, Z. L. Wang, *Science* **2008**, *322*, 238.
[18] E. Cheung, M. Sitti, *Langmuir* **2009**, *25*, 6613.
[19] H. Lee, B. P. Lee, P. B. Messersmith, *Nature* **2007**, *448*, 338.
[20] H. E. Jeong, M. K. Kwak, K. Y. Suh, *Langmuir* **2010**, *26*, 2223.
[21] Y. Menguc, S. Y. Yang, S. Kim, J A. Rogers, M. Setti, *Adv. Func. Mater.* **2012**, *22*, 1246.
[22] M. K. Kwak, H. E. Jeong, W. G. Bae, H. Jung, K. Y. Suh, *Small* **2011**, *7*, 2296.
[23] D. Paretkar, M. Kamperman, A. S. Schneider, D. Martina, C. Creton, E. Arzt, *Mat. Sci. Eng. C* **2011**, *31*, 1152.
[24] K. Jin, Y. Tian, J. S. Erickson, J. Puthoff, K. Autumn, N. S. Pesika, *Langmuir* **2012**, *28*, 5737.
[25] R. Spolenak, S. Gorb, E. Arzt, *Acta Biomaterialia* **2005**,*1*, 5.
[26] K. Kendall, *J. Phys. D* 1975, *8*, 1449.
[27] N. S. Pesika, Y. Tian, B. X. Zhao, K. Rosenberg, H. B. Zeng, P. McGuiggan, K. Autumn, J. N. Israelachvili, *J. Adhesion* **2007**, *83*, 383.
[28] S. Kim, M. Spenko, S. Trujillo, B. Heyneman, D. Santos, M. R. Cutkosky, *IEEE Trans. Robot.* **2008**, *24*, 65.
[29] J. Krahn, Y. Liu, A. Sadeghi, C. Menon, *Smart Mater. Struct.* **2011**, *20*, 115021.
[30] E. Kroner, R. Maboudian, E. Arzt, *Adv. Eng. Mat.* **2010**, 12, 398.